IJISET - International Journal of Innovative Science, Engineering & Technology, Vol. 3 Issue 12, December 2016
ISSN (Online) 2348 – 7968 | Impact Factor (2015) - 4.332
www.ijiset.com

3D study of a Polycrystalline Bifacial Silicon Solar Cell, Illuminated Simultaneously by Both Sides: Grain Size and Recombination Velocity Influence.

Omar MBAO[1], Moustapha THIAME[1], Ibrahima Ly[2], Ibrahima DATTA[1], Marcel .S. DOUF[1], Youssou TRAORE[1], Mor NDIAYE[1] And Grégoire SISSOKO[1]

[1]Laboratoire des Semi-conducteurs et d'Energie Solaire, Faculté des Sciences et Techniques, Université Cheikh Anta Diop, Dakar, Sénégal

[2]Ecole Polytechnique de Thiès, Sénégal

Abstract

In this work, for simultaneous illumination of both sides of the polycrystalline bifacial silicon solar cell, we study the influence of grain size and recombination velocity at grain boundaries, on the macroscopic and microscopic parameters. The study allows us understandind why the carrier density, current density and photovoltage have lower values than those collected on the monocrystalline Si when the solar cell is illuminated simultaneously by both sides.
It highlighted the electrical parameters degradation of the solar cell as photocurrent, short-circuit current, photovoltage and open circuit voltage, when grain size decreases or when recombinations at grain boundaries are high.

Keywords

"polycrystalline Si" "simultaneous illumination" "carrier density" "current density" "photovoltage" "recombination velocity" "grain size"

1. INTRODUCTION

In order to improve the quality of solar cells, many studies have been conducted on the polycrystalline Si in order to control the photovoltaic conversion.
The latter is governed by the processes as the generation of electron-hole pairs, their diffusion and recombination [1,2]. So it is limited by the presence of the Si material manufacturing defects which mastery would increase the cell efficiency.
Among these defects, we have the grain boundaries formed among silicon crystals that are responsible, among other, of charge carriers recombination photogenerated in volume **[3-5].**
The objective of this study is to analyze the influence of recombination at grain boundaries and the crystal size called grain on the electrical parameters of the polycrystalline Si solar cell. Thus, from a 3D modeling, we will determine an expression of the minority carriers density in the base when the solar cell is illuminated simultaneously by both sides by a constant multispectral light.
This expression of the carrier density will allow us to determine the expression of the photocurrent, the photovoltage, the short-circuit current, the open circuit voltage, the back surface recombination velocity, and study the influence of grain boundaries recombination and grain size on these parameters.

2. THEORITICAL ANALYSIS

The BSF polycrystalline silicon solar cell studied is an n^+-p-p^+ structure as shown in figure 1.a. Silicon consisting of several grain of various sizes, for our study, we use the 3D columnar model where each grain has a rectangular shape as shown in figure1.b below **[3,6,7].**

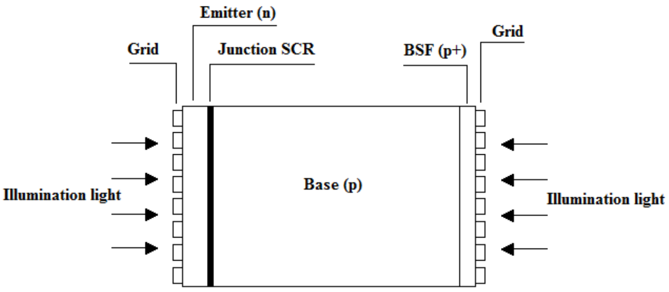

Figure 1.a. Bifacial Silicon solar cell Structure

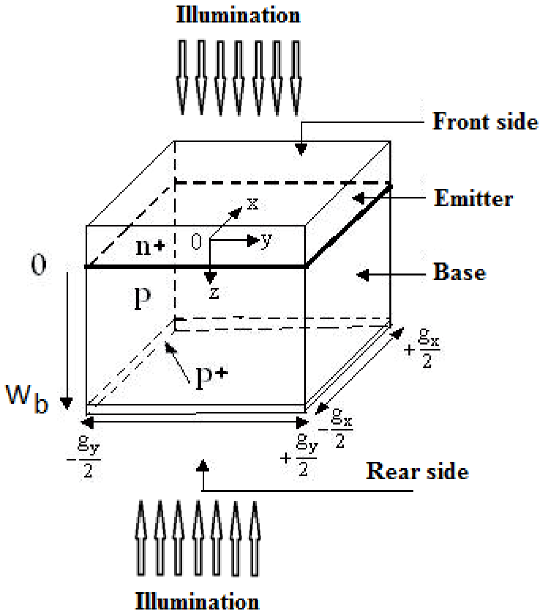

Figure 1.b : Polycristalline Silicon columnar grain model

In this study, we assume that:

- the contribution of the emitter is neglected. We take into account only the base contribution **[3],**
- the illumination is uniform. We then have a generation rate depending only with base depth *z* **[8]**;
- the existing crystalline field within the base is neglected
- in the simulation, we have equality between the grain size along x and y axes, ie gx = gy = g(square cross section), and that the recombination velocity at grain boundaries is perpendicular to the junction and independent to the generation rate under AM 1.5 **[3,9].**

For both side simultaneous illumination of the solar cell with a constant multispectral light, excess carriers in the base of the solar cell are governed by the following continuity equation:

$$\frac{\partial^2\delta(x,y,z)}{\partial x^2}+\frac{\partial^2\delta(x,y,z)}{\partial y^2}+\frac{\partial^2\delta(x,y,z)}{\partial z^2}=\frac{\delta(x,y,z)}{L^2}-\frac{1}{D}\sum_{i=1}^{3}a_i\cdot\left\{\exp(-b_i\cdot z)+\exp(-b_i\cdot(wb-z))\right\} \quad (1)$$

In this equation: L is the diffusion length, D the diffusion coefficient, a_i and b_i the solar radiation tabulated values and the dependence of silicon absorption coefficient with wavelength for AM = 1.5 **[10,11].**

A general solution of the continuity equation (1) can be expressed as **[3,9]:**

$$\delta(x,y,z)=\sum_k\sum_j Z_{k,j}(z)\cdot\cos(c_k x)\cos(c_j y) \quad (2)$$

where *ck* and *cj* are values obtained from the following grain boundary conditions at $\pm\frac{gx}{2}$ and $\pm\frac{gy}{2}$ **[2 ,3]:**

$$\left[\frac{\partial\ \delta(x,y,z)}{\partial x}\right]_{x=\pm\frac{gx}{2}}=\mp\frac{Sgb}{D}\cdot\delta(\pm\frac{gx}{2},y,z) \quad (3)$$

$$\left[\frac{\partial\ \delta(x,y,z)}{\partial y}\right]_{x=\pm\frac{gx}{2}}=\mp\frac{Sgb}{D}\cdot\delta(x,\pm\frac{gy}{2},z) \quad (4)$$

Equations (3) and (4) define a grain boundary recombination velocity *Sgb* that traduces how excess carriers flow trough grain boundaries; *gx* and *gy* are the grain sizes according to x and y axis.

Replacing *δ*(*x, y, z*) by its expression into the above two boundary conditions lead to the following transcendental equations:

$$c_k \cdot \tan(c_k \cdot \frac{gx}{2}) = \frac{Sgb}{D} \quad (5)$$

$$c_j \cdot \tan(c_j \cdot \frac{gy}{2}) = \frac{Sgb}{D} \quad (6)$$

c_k and c_j are eigen values of these transcendental equations solved graphically. Replacing $\delta(x, y, z)$ in the continuity equation and using the fact that the cosine functions are orthogonal we obtain the following expression of $Z_{k,j}(z)$:

$$Z_{k,j}(z) = O_{k,j} \cdot ch(\frac{z}{L_{k,j}}) + P_{k,j} \cdot sh(\frac{z}{L_{k,j}}) - \sum_{i=1}^{3} K_i \cdot \{\exp(-b_i \cdot z) + \exp(-b_i \cdot (wb - z))\} \quad (7)$$

In this expression :

$$L_{k,j} = \left[c_k^2 + c_j^2 + L^{-2}\right]^{-\frac{1}{2}} \quad (8)$$

$$K_i = \frac{L_{k,j}^2}{D_{k,j} \cdot \left[b_i^2 \cdot L2_{k,j} - 1\right]} \cdot a_i \quad (9)$$

and

$$D_{k,j} = \frac{D \cdot \left[\sin(c_k \cdot gx) + c_k \cdot gx\right] \cdot \left[\sin(c_j \cdot gy) + c_j \cdot gy\right]}{16 \cdot \sin(c_k \cdot \frac{gx}{2}) \cdot \sin(c_j \cdot \frac{gy}{2})} \quad (10)$$

Constants $O_{k,j}$ and $P_{k,j}$ are calculated by mean of the boundary conditions **[3, 11, 13]**:

at the n^+-p surface ($z = 0$):

$$\left[\frac{\partial \delta(x,y,z)}{\partial z}\right]_{z=0} = \frac{Sf}{D} \cdot \delta(x,y,0) \quad (11)$$

at the back surface ($z = wb$)

$$\left[\frac{\partial \delta(x,y,z)}{\partial z}\right]_{z=wb} = -\frac{Sb}{D} \cdot \delta(x,y,wb) \quad (12)$$

In these expressions, Sf represents the minority carrier junction recombination velocity. It quantifies how excess carrier flow through the junction in actual operating conditions. *Sb* is the effective back surface recombination velocity. It quantifies the rate at which excess minority carriers are lost, at the back surface of the cell **[11,15].**

We obtain:

$$O_{k,j} = \sum_{i=1}^{3} K_{k,j} \cdot \frac{Y_{k,j} \cdot (\frac{Sf}{D} + b_i) + \frac{1}{L_{k,j}} \cdot (\frac{Sb}{D} + b_i) + \left[Y_{k,j} \cdot (\frac{Sf}{D} - b_i) + \frac{1}{L_{k,j}} \cdot (\frac{Sb}{D} - b_i)\right] \cdot \exp(-b_i \cdot wb)}{\frac{Sf}{D} \cdot Y_{k,j} + \frac{X_{k,j}}{L_{k,j}}} \quad (13)$$

$$P_{k,j} = \sum_{i=1}^{3} K_{k,j} \cdot \frac{\frac{Sf}{D} \cdot (\frac{Sb}{D} + b_i) - X_{k,j} \cdot (\frac{Sf}{D} + b_i) + \left[\frac{Sf}{D} \cdot (\frac{Sb}{D} - b_i) - X_{k,j} \cdot (\frac{Sf}{D} + b_i)\right] \cdot \exp(-b_i \cdot wb)}{\frac{Sf}{D} \cdot Y_{k,j} + \frac{X_{k,j}}{Y_{k,j}}} \quad (14)$$

with :

$$X_{k,j} = \frac{1}{L_{k,j}} \cdot sh(\frac{wb}{L_{k,j}}) + \frac{Sb}{D} \cdot ch(\frac{wb}{L_{k,j}}) \text{ and } Y_{k,j} = \frac{1}{L_{k,j}} \cdot ch(\frac{wb}{L_{k,j}}) + \frac{Sb}{D} \cdot sh(\frac{wb}{L_{k,j}}) \quad (15) \text{ and } (16)$$

2. RESULTS ET DISCUSSIONS

2.1. Excess minority carrier density

Figures 2 and 3 present profiles of excess minority carrier density as a function of base depth, respectively for different grain boundaries recombination velocity and different grain size.

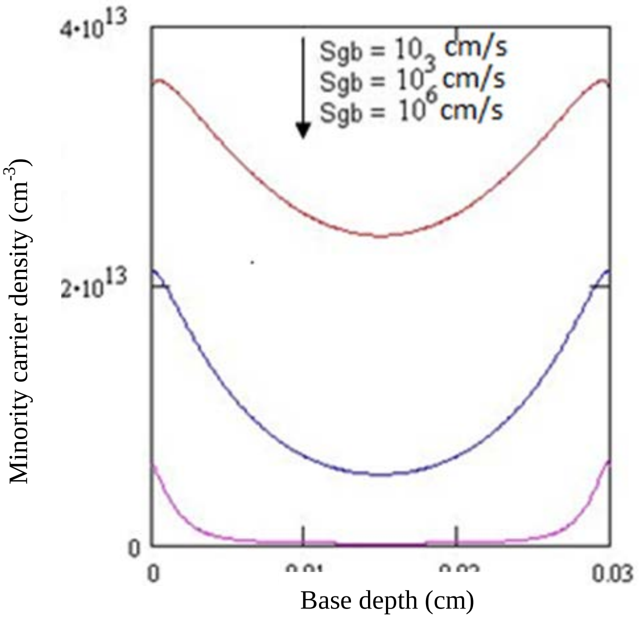

Figure (2) : Profile of the excess minority carrier density as a function of depth z in the base for different Sgb; g=0.005cm, $Sf=3\cdot10^3 cm/s$, $Sb=3\cdot10^3 cm/s$ $wb=0.03cm$ and AM1.5

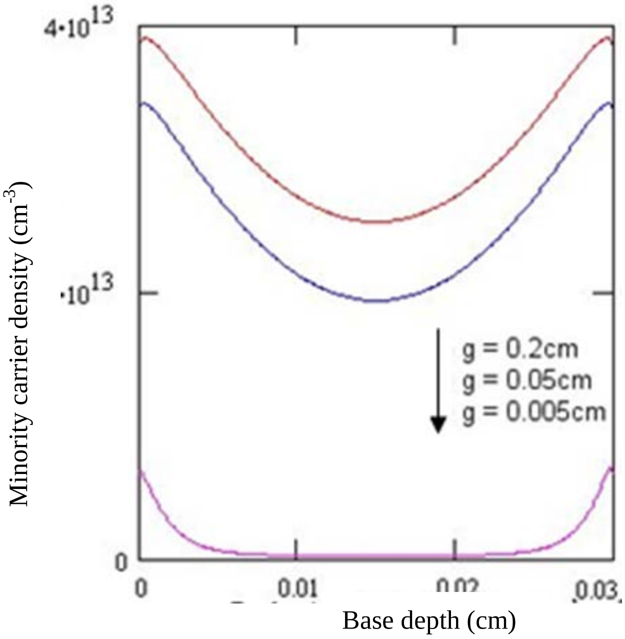

Figure 3 : Profile of the excess minority carrier density as a function of depth z in the base for differ rent grain sizes; $Sgb=10^5$ cm/s ; $Sf=3\cdot10^3 cm/s$; $Sb=3\cdot10^3 cm/s$; $wb=0.03cm$ and AM1.5.

These figures show that for simultaneous illumination of the solar cell by both front and back sides, the minority carrier density in the base decreases when moving deeply in the base. A maximum of carriers is photogenerated in these sides. The carrier density is low when approaching the center of the base **[3,16],** according to Fick law for thick base depth effect.

These profiles also highlight the effect of the grain size and grain boundaries recombination on the carrier density. The decrease in the grain size causes a decrease of the carrier density **[3]**. Indeed, the reduction in grain size leads to an increase of recombination centers at the grain boundaries.

We also note that the higher the recombination velocity at the grain boundaries, the more the carrier density is small. This variation highlights the effect of recombination at the joints.

2.2. Photocurrent density

From the expression of the minority carriers density in the base, we obtain the expression of the photocurrent density from the following relationship **[3,15,17]** :

$$J=\frac{q\cdot D}{gx\cdot gy}\int_{-\frac{gx}{2}}^{+\frac{gx}{2}}\int_{-\frac{gy}{2}}^{+\frac{gy}{2}}\left[\frac{\partial\delta(x,y,z)}{\partial z}\right]_{z=0}\cdot dx\cdot dy \quad (17)$$

After calculation we get:

$$J=q\cdot D\cdot\sum_k\sum_j R_{k,j}\cdot\left(\frac{P_{k,j}}{L_{k,j}}+\sum_{i=1}^{3}K_{k,j}\cdot b_i\cdot\left[1-\exp(-b_i\cdot wb)\right]\right) \quad (18)$$

with $$R_{k,j}=\frac{4\cdot\sin(\frac{c_k\cdot gx}{2})\cdot\sin(\frac{c_j\cdot gy}{2})}{gx\cdot gy\cdot c_k\cdot c_j} \quad (19)$$

We plot at figures 4 and 5 the photocurrent density profiles as a function of junction recombination velocity, respectively for different grain sizes and different grain boundaries recombination velocities.

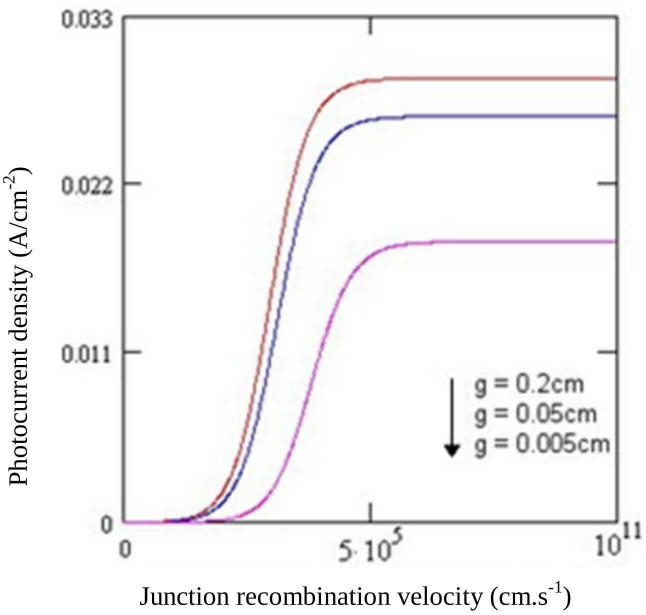

Figure 4: Profile of the photocurrent density versus recombination velocity at the junction for different grain sizes; $Sgb = 10^5$ cm/s ; $Sb = 3 \cdot 10^3 cm/s$; $wb = 0.03 cm$ and AM1.5

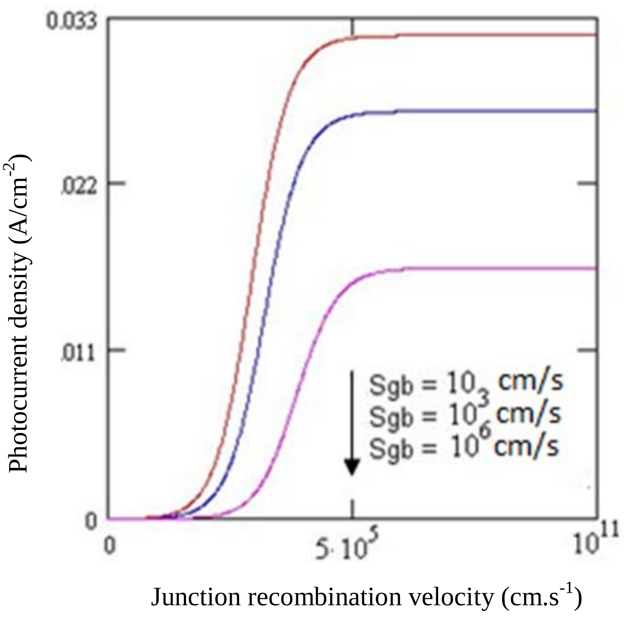

figure 5 : Profile of the excess minority carrier density versus junction recombination velocity for different Sgb ; g=0.005cm, $Sb = 3 \cdot 10^3 cm/s$, $wb = 0.03 cm$ and AM1.5

The profiles show that the photocurrent density have two levels: the first corresponding to the solar cell in open circuit mode is obtained for low junction recombination velocity (lower to 2.10^2cm / s); the second corresponding to the solar cell in short circuit mode is obtained when Sf is higher than 5.10^5 cm/s. Between these two levels, the photocurrent density increases progressively with Sf, which corresponds to different operating points of the solar cell **[3].**

The photocurrent density highly decreases when the grain size decreases and when the recombination velocity at the grain boundaries increases.

These figures therefore emphasize the degradation of the photocurrent density when the recombination centers are important in the solar cell base substrate.

2.3. Short circuit current

The short circuit current density Jsc is obtained from the photocurrent density for large values of the recombination velocity at the junction [3,11].
It is given by the following expression

$$Jsc = \lim_{Sf \geq 5.10^5 \, cm/s} J \qquad (20)$$

After calculation, we obtain an expression of the short-circuit current density when the solar cell is illuminated simultaneously by both sides:

$$Jcc = q \cdot D \cdot \sum_k \sum_j \left(\frac{R_{k,j}}{L_{k,j}} \cdot \sum_{i=1}^{3} K_{k,j} \cdot \left[\frac{1}{Y_{k,j}} \cdot \left(\frac{Sb}{D} + b_i\right) - \frac{X_{k,j}}{Y_{k,j}} + b_i \cdot L_{k,j} \right] + \left[\frac{1}{Y_{k,j}} \cdot \left(\frac{Sb}{D} - b_i\right) - \frac{X_{k,j}}{Y_{k,j}} - b_i \cdot L_{k,j} \right] \cdot \exp(-b_i \cdot wb) \right) \qquad (21)$$

Figures 6 and 7 highlight the influence of the grain size and the recombination velocity at the joints on the short-circuit current density.

IJISET - International Journal of Innovative Science, Engineering & Technology, Vol. 3 Issue 12, December 2016
ISSN (Online) 2348 – 7968 | Impact Factor (2015) - 4.332
www.ijiset.com

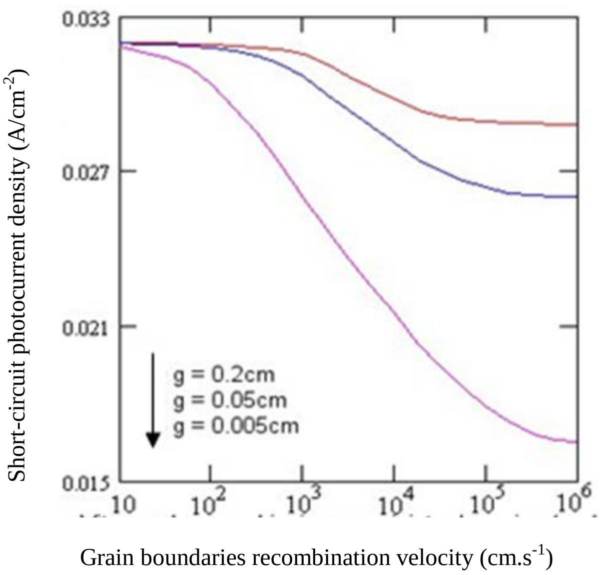

Figure 6: Profile of the short-circuit current density versus recombination velocity at the grain boundaries for different grain size, with $Sf = 5.10^5 cm/s$, $Sb = 3.10^3 cm/s$ $wb = 0.03 cm$ and AM1.5.

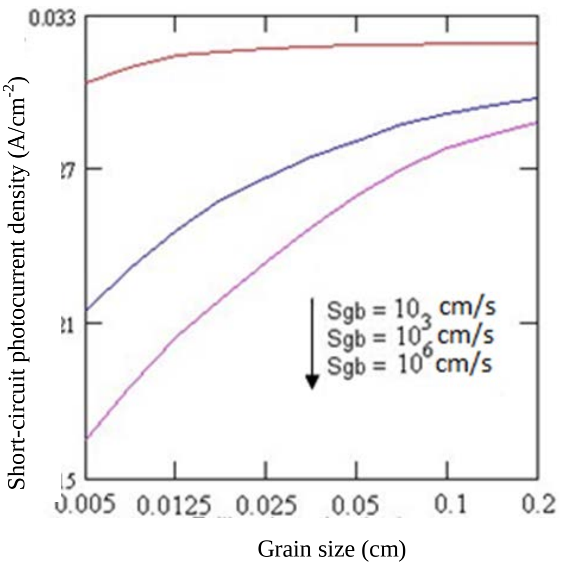

Figure 7: Profile of the short-circuit current density versus grain size for different recombination velocity at the grain boundaries, with $Sf = 5.10^5 cm/s$, $Sb = 3.10^3 cm/s$ $wb = 0.03 cm$ and AM1.5.

These profiles show that the short circuit current density generally decreases as the recombination velocity at the grain boundaries increases. It considerably increases as the grain size increases.

Recombination at grain boundaries have a powerful influence on the short-circuit current when the grain size is small.

For large grain size and low recombination velocities, the short-circuit current is almost constant and is substantially equal to that delivered by a monocrystalline solar cell simultaneously illuminated by both sides **[9]**.

2.4. Photovoltage

It is obtained using the Boltzmann relation **[3,17]**:

$$V = V_T \cdot \log\left[1 + \frac{N}{n_i^2} \cdot \int_{-\frac{gx}{2}}^{+\frac{gx}{2}} \int_{-\frac{gy}{2}}^{+\frac{gy}{2}} \delta(x, y, 0)\right] \quad (22)$$

When the photocell is illuminated simultaneously by the front and rear sides, the photovoltage is given by the following expression :

$$V = V_T \cdot \ln\left\{1 + \frac{N}{n_i^2} \cdot \sum_k \sum_j R_{k,j}\left[O_{k,j} - \sum_{i=1}^{3} K_{k,j} \cdot (1 + \exp(-b_i \cdot wb))\right]\right\} \quad (23)$$

In figures 4 and 5, we plot photovoltage profiles versus recombination velocity at the junction, respectively for different grain boundaries recombination velocities and grain sizes.

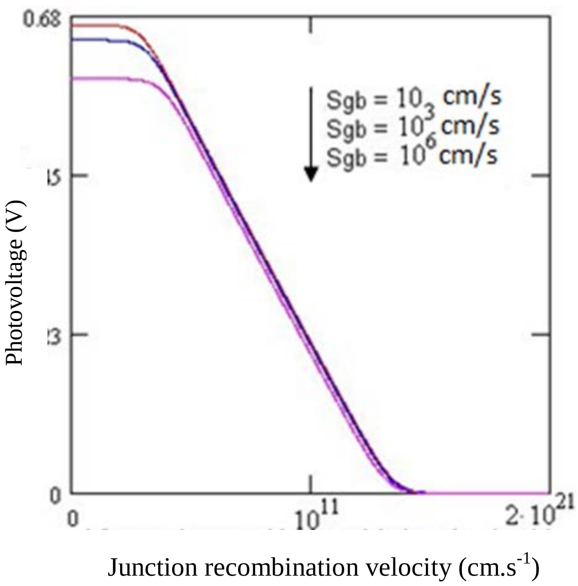

Figure 8: Profile of photovoltage versus recombination velocity at the junction for different recombination velocities at the grain boundaries: *g=0.005cm*, $Sb = 3\cdot10^3 cm/s$ $wb = 0.03cm$ *and AM1.5.*

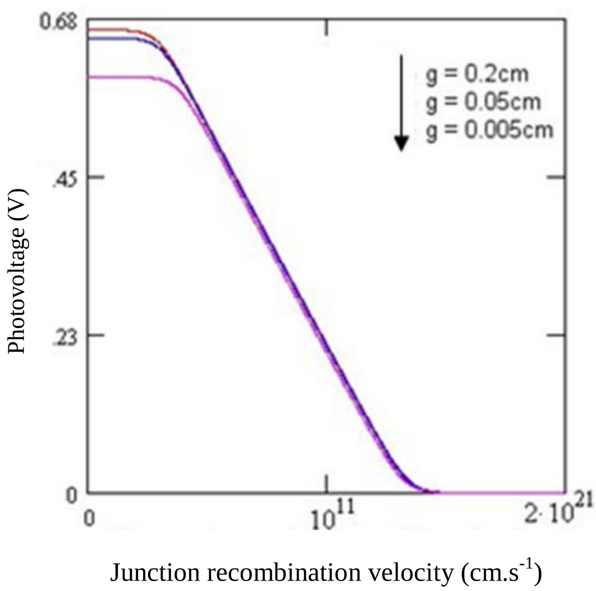

Figure 9: Profile of the photovoltage versus recombination velocity at the junction for different grain sizes : $Sgb{=}10^5$ *cm/s,* $Sb{=}3{\cdot}10^3 cm/s$, $wb{=}0.03cm$ *and AM1.5.*

The profiles show that the photovoltage has a horizontal bearing for low values of the recombination velocity at the junction (Sf $\leq 2.10^2$cm / s). In this area, the voltage is maximum, which corresponds to an open circuit mode of the solar cell. It then decreases when Sf increases.
There is also an overall decrease in the photovoltage when the recombination velocity at grain boundaries increases and when the grain size decreases. The effect of grain size and Sf on the photovoltage occurs more for low Sf values(open circuit).

2.5. Open circuit photovoltage

In open circuit, the recombination velocity at the junction tends to zero. So we get the expression of the open circuit photovoltage in exploiting the following equation **[3,11]**:

$$Vco = V(Sf \leq 2.10^2 cm/s) \qquad (24)$$

Expression of this open circuit voltage for simultaneous illumination by both sides is given by:

$$Vco = V_T \cdot \ln\left\{1+\frac{N}{n_i^2}\cdot\sum_k\sum_j R_{k,j}\cdot\left(\sum_{i=1}^{3} K_{k,j}\cdot\left[\frac{1}{X_{k,j}}\cdot(\frac{Sb}{D}+b_i)+\frac{Y_{k,j}}{X_{k,j}}\cdot b_i\cdot L_{k,j}-1\right]+\left[\frac{1}{X_{k,j}}\cdot(\frac{Sb}{D}+b_i)+\frac{Y_{k,j}}{X_{k,j}}\cdot b_i\cdot L_{k,j}-1\right]\cdot\exp(-b_i\cdot wb)\right)\right\} \qquad (25)$$

Figures 10 and 11 represent the profile of the open circuit photovoltage versus respectivly the recombination velocity for different grain sizes and the grain size for different grain boundaries recombination velocity. They highlight the influence of grain size and recombination at grain boundaries on the open circuit voltage.

IJISET - International Journal of Innovative Science, Engineering & Technology, Vol. 3 Issue 12, December 2016
ISSN (Online) 2348 – 7968 | Impact Factor (2015) - 4.332
www.ijiset.com

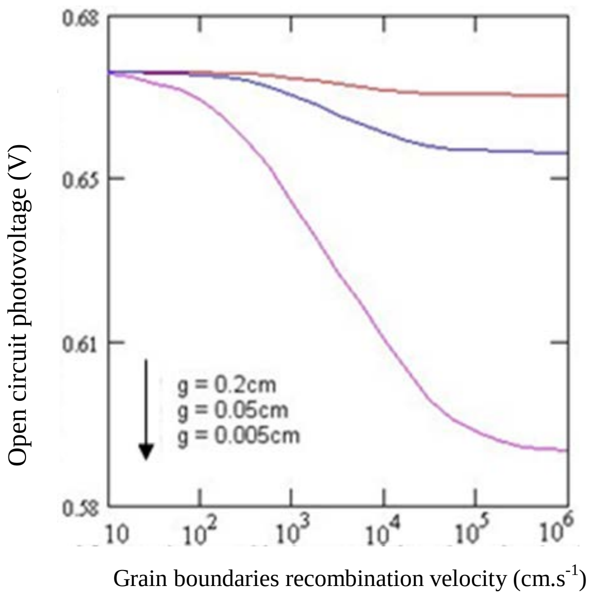

Figure 10: Profile of the open-circuit photovoltage versus grain boundaries recombination velocity for different grain sizes; $Sf = 2\cdot 10^2 cm/s$, $Sb=3\cdot 10^3 cm/s$ $wb=0.03cm$ and AM1.5.

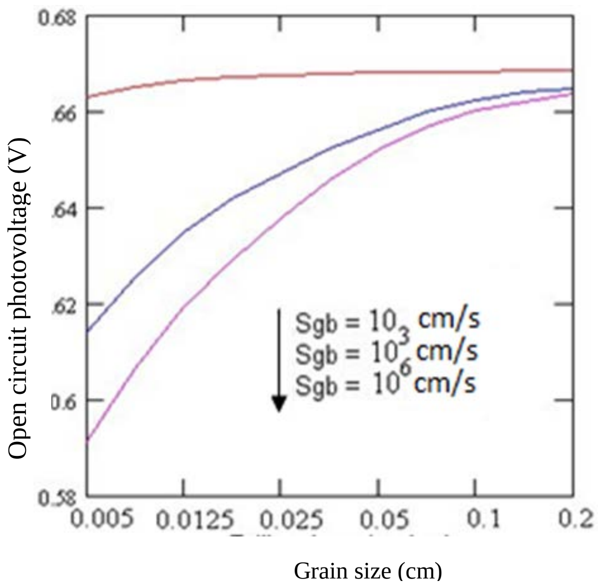

Figure 11: Profile of the open-circuit photovoltage versus grain size for different grain boundaries recombination; $Sf = 2\cdot 10^2 cm/s$, $Sb=3\cdot 10^3 cm/s$ $wb=0.03cm$ and AM1.5.

The open-circuit photovoltage decreases according to the recombination velocity at the grain boundaries. This decrease is even more remarkable when the grain size is small. The quality of the solar cell deteriorates when the grain size is small.

2.6 . Current - voltage characteristics

The current - voltage characteristic is obtained by plotting current density J(sf) versus photovoltage V(sf) [19].

In this section we study the influence of grain size and grain boundaries recombination velocity on the current-voltage characteristic.

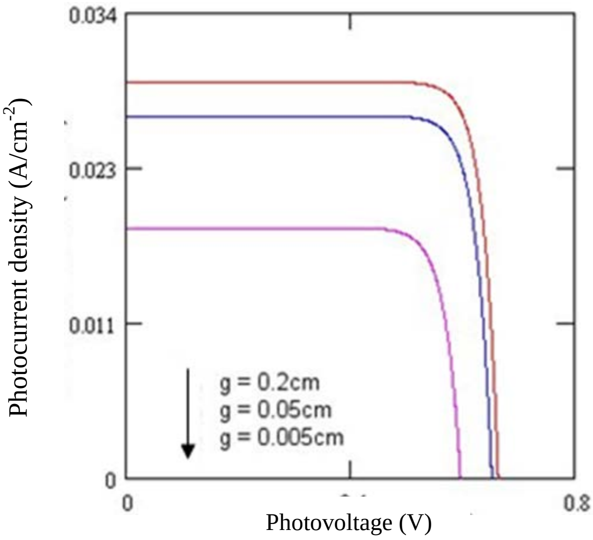

Figure 12: Current - voltage characteristic for different grain sizes with $Sgb=10^5$ cm/s, $Sb=3\cdot 10^3 cm/s$ $wb=0.03cm$ *and AM1.5*

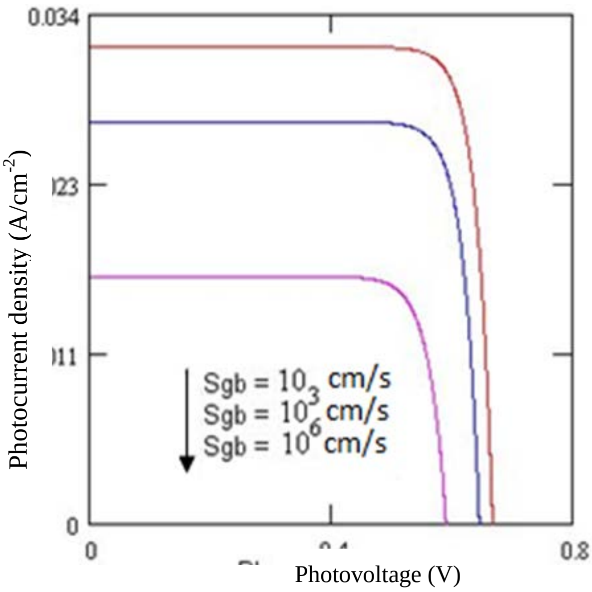

Figure 13: Current - voltage characteristic for different values of Sgb, *g=0.005cm and for,* $Sb=3\cdot 10^3 cm/s$, $wb=0.03cm$ *and AM1.5.*

When the photovoltage is zero, the photocurrent corresponds to the short-circuit current and when the current tends to zero, the voltage is the open circuit one. Figure 12 represent the current-voltage characteristic for different grain sizes. It generally decreases as grain size decreases [2, 20, 21].

Figure 13 which corresponds to the profile of current-voltage characteristics for different grain recombination velocities, shows an overall decrease in voltage and photocurrent when grain boundaries recombination increases [2, 22].

When the grain size decreases from 0.2 cm to 0.005 cm, there is a decrease of the short circuit current of approximately 45% and a reduction of the voltage in open circuit by approximately 15%. As regards the recombination velocity at the grain boundaries, an increase from 10 cm/s to 10^3 cm/s, causes a reduction of the short-circuit current of about 40% and a decrease in the open circuit voltage about 15%. This confirms the deterioration of the quality of the solar cell in the presence of many grain boundaries **[20,22]**.

3.4. Recombination parameters: back surface recombination velocity Sb.

For illumination of the solar cell simultaneously by the front and back, we have previously noted a strong presence of charge carriers near the back surface. This will be the headquarters of strong recombination of photocreated carriers [3]. Control back surface recombinant parameters would be useful to improve the quality of bifacial photovoltaic cells.

Thus, to determine the back surface recombination velocity, we consider that the current density is the sum of many small current densities $J_{k,j}$, depending on the solutions of transcendental equations (5) and (6)**[3]**

$$J = \sum_k \sum_j J_{k,j} \qquad (26)$$

with :

$$J_{k,j} = q \cdot R_{k,j} \cdot Sf \cdot \sum_{i=1}^{3} K_{k,j} \cdot \frac{\dfrac{Sb - D \cdot b_i}{D \cdot Y_{k,j}} \cdot \exp(-b_i \cdot wb) - \dfrac{X_{k,j}}{Y_{k,j}} + b_i \cdot L_{k,j}}{\dfrac{X_{k,j}}{Y_{k,j}} + \dfrac{Sf \cdot L_{k,j}}{D}} \qquad (27)$$

Knowing that the photocurrent density has a horizontal bearing for very large values of the recombination velocity at the junction Sf , we can write**[**3,11,21**]**:

$$\left(\frac{\partial J}{\partial Sf}\right)_{Sf \geq 5.10^5 cm/s} = 0 \qquad (28)$$

We thus have a new expression of $Sb_{k,j}$ that describes how the minority carriers in the base recombine at the back surface when the solar cell is illuminated simultaneously by both sides with a constant multispectral light, with a recombination velocity depending on c_k and c_j solutions of transcendental equations (5) and (6).

$$Sb_{k,j} = \frac{D}{L_{k,j}} \cdot \frac{\sum K_i \cdot \left[\left(b_i \cdot L_{k,j} \cdot \cosh(\frac{wb}{L_{k,j}}) + \sinh(\frac{wb}{L_{k,j}}) + b_i \cdot L_{k,j}\right) \cdot \exp(-b_i \cdot wb) - b_i \cdot L_{k,j} + \sinh(\frac{wb}{L_{k,j}}) - b_i \cdot L_{k,j} \cdot \cosh(\frac{wb}{L_{k,j}})\right]}{\sum K_i \cdot \left[\left(1 - \cosh(\frac{wb}{L_{k,j}}) - b_i \cdot L_{k,j} \cdot \sinh(\frac{wb}{L_{k,j}})\right) \cdot \exp(-b_i \cdot wb) + 1 - \cosh(\frac{wb}{L_{k,j}}) + b_i \cdot L_{k,j} \cdot \sinh(\frac{wb}{L_{k,j}})\right]}$$

(29)

Figure 14 represent its profile versus the recombination velocity at the grain boundaries for different grain size.

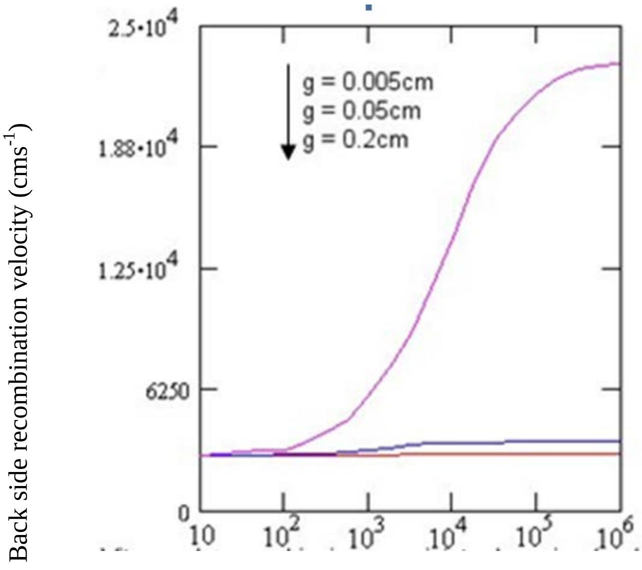

Figure 14: Profile of the back surf velocity at grain boundaries for different grain sizes; $wb=0.03cm$ and AM1.5.

Profiles highlight an increase in the back surface recombination velocity when the recombination velocity at grain boundaries increases. This increase is more remarkable when the grain size is small. For high values of grain size, the back surface recombination is almost independent of recombination at grain boundaries [3].
The low grain sizes correspond to a massive presence of grain boundaries on the rear with a consequent increase in recombination of carriers photogenerated at back surface.

CONCLUSION

Considering the 3D columnar grain model of the polycrystalline silicon, we have studied the influence of recombination velocity at grain boundaries and the grain size on the parameters of the polycrystalline bifacial silicon solar cell as the density of carriers, the photocurrent, the photovoltage, the short-circuit current, the open circuit voltage and the back surface recombination velocity. The study allowed assessing the degradation of these parameters when grain size decreases or when recombination at grain boundaries increases. It helps in understanding the difference between monocristalline and polycrystalline silicon.
It also enables to see when going from low grain sizes to large grain size, we have a strong reduction in recombination of carriers in the base, because the grain boundaries which are recombination centers in the substrate decrease.

References

[1] Ryuichi Shimokawa and Yutaka Hayachi
Effect of localized grain boundaries in semicrystalline silicon salar cells J. Appl. Phys. ,Vol. 59, N°7. Pp 2571-2576, (1986)

[2] M.C. HALDER and T.R. WILLIAMS Grain boundary effects in polycrystalline silicon solar cells I: Solution of the three dimensional diffusion equation by the green's function method Solar Cells, Vol. 8, Pp 201-223, (1983)

[3] H. L. Diallo, A. Wereme, A. S. Maïga and G. Sissoko:
New approach of both junction and back surface recombination velocities in a 3D modeling study of a polycrystalline silicon solar cell. Eur. Phys. J. Appl. Phys., 42: (2008), pp.203–11.

[4] S.C. Jain The effective lifetime in semicrystalline silicon Solar Cells, Vol. 9, Pp 345-352, (1983)

[5] J. Oualid, M. Bonfils, J P Crest G. Mathian H Amzil, J. Dugas, M. Zehaf AND S. Martinuzzi Photocurrent and Diffusion Lengths at the Vicinity of Grain Boundaries (g.b.) in N and P-type Polysilicon. Evaluation of the g.b. Recombination Velocity Revue Phys. Appl. 17, (1982), pp119-124

[6] S. R. Dhariwal Photocurrent and photovoltage from polycrystalline p-n junction solar cells Solar Cells, Vol. 25, pp 223-233, (1988)

[7] H. El GHITANI and S. MARTINUZZI Influence of dislocations on electrical properties of large grained polycrystalline silicon cells. I. Model J. Appl. Phys. ,Vol. 66, N°4. Pp 1717-1722, (1989)

[8] MUZEYYEN SARITAS and HARRY D. MCKELL ,Comparison of Minority-Carrier Diffusion Length Measurements in Silicon by the Photoconductive Decay and Surface Photovoltage Methods, J. Appl. Phys. 63 (9), (1988),pp4561-4567

[9] J. DUCAS; 3D Modelling of a Reverse Cell Made with Improved Multicrystalline Silicon Wafer. Solar Energy Materials & Solar Cells, 32, (1994) pp. 71-88

[10] S.N. Mohammad:An alternative method for the performance analysis of silicon solar cells, J. Appl. Phys., LXI (2), (1987) pp.767–772

[11] G. Sissoko, E. Nanema, A. Correa, M. Adj, A.L. Ndiaye, M.N. Diarra Recombination parameters measurement in double sided surface field solar cell Proceedings of World Renewable Energy Conference, Florence–Italy (1998), pp. 1856–1859

[12] Mayoro Dieye, Senghane Mbodji, Martial Zoungrana, Issa Zerbo, Biram Dieng, Gregoire Sissoko; A 3D Modelling of Solar Cell's Electric Power under Real Operating Point; World Journal of Condensed Matter Physics, (2015), 5, 275-283

[13]: G. Sissoko, C. Museruka, A. Correa, I. Gaye and A.L. Ndiaye, *Light SpectralEffect on Recombinaison Parameters of Silicon Solar Cell*', Proceedings of the World Renewable Energy Congress, Denver-USA, Part III,(1996),pp.1487- 1490

[14] M.C. HALDER and T.R. WILLIAMS Grain boundary effects in polycrystalline silicon solar cells I: Solution of the three dimensional diffusion equation by the green's function method Solar Cells, Vol. 8, Pp 201-223, (1983)

[15]: M. M. Dione, I. Ly, A. Diao, S. Gueye, A. Gueye, M. Thiame, G. Sissoko;

[20] Mbodji, S., Mbow, B., Barro, F.I. and Sissoko, G: A 3D Model for Thickness and Diffusion Capacitance of Emitter-Base Junction Determination in a Bifacial Polycrystalline Solar Cell under Real Operating Condition. *Turkish Journal of Physics*, **15**, (2011) pp. 281-291

[21] G. Sissoko, E. Nanéma, A. L. Ndiaye, Y. L. B. Bocandé and M. Adj.Minority carrier diffusion length measurement in silicon solar cell under constant white bias light. Renewable Energy, Vol 3, pp.1594-1597, 1996.- Pergamon, 0960-1481

[22]M. M. DIONE, A. DIAO, M. NDIAYE, H. LY DIALLO, N. THIAM, F. I. BARRO, M. WADE, A. S. MAIGA, G. SISSOKO: 3D Study Of A Monofacial Silicon Solar Cell Under Constant monocrhomatic Light: Influence Of Grain Size, Grain Boundary Recombination Velocity, Illumination Wavelength, Back Surface And Junction Recombination Velocities; Proceeding of 25th European Photovoltaic Solar Energy Conference and Exhibition 5th World Conference on Photovoltaic Energy Conversion (2010), pp. 488-491

Determination of the impact of the grain size and the recombination velocity at grain boundary on the values of the electrical parameters of a bifacial polycristallin silicon solarcell",
IRACST – Engineering Science and Technology: International Journal, Vol.3, No.1, (2013), pp. 66-73

[16]: Daniel L. Meier, Jeong-Mo Hwang and Robert B. Campbell The effect of doping density and injection level on minority-carrier lifetime as applied to bifacial dendritic web silicon solar cells IEEE TRANSACTIONS ON ELECTRON DEVICES, Vol. ED-35, N^{O}1, pp 70-79,(1988)

[17] ADEL BEN ARAB, Photovoltaic properties and high efficiency of preferentially doped polysilicon solar cells Solid-State Electronics, Vol. 38, N°8, (1995) Pp 1441-1447

[18] B. BA, M. KANE, A. FICKOU and G SISSOKO Excess minority carrier densities and transient short circuit currents in polycrystalline silicon solar cells; Solar Energy Materials and Solar Cells, 31 (1993), pp.33-49

[19] Y. L. B. Bocande, A. Correa, I. Gaye, M. L. Sow and G. Sissoko Bulk and surfaces parameters determination in high efficiency Si solar cells. Renewable Energy, vol 5, part III, pp. 1698-1700, 1994- Pergamon, 0960-1481